CHAPTER 3

MORPHOLOGY AND MECHANICAL PROPERTIES OF COPPER-GRAPHITE-TiC COMPOSITES

3.1 INTRODUCTION

This chapter focuses on the fabrication of composites with different wt.% of TiC particles through powder metallurgy technique and also includes the optimization of sintering time and temperature. The interpretations of XRD analysis of pure copper and composites for phase identification are also shown. The Cu-Gr-TiC composites have been characterized by different techniques and the influence of varying wt.% of TiC particles on microstructure, physical, and mechanical properties of composites is presented and discussed.

3.2 EFFECT OF SINTERING ON COPPER-GRAPHITE COMPOSITE

The ball milled Cu-5wt.% Gr powders were compacted using a punch die arrangement. Further, the green compact was sintered at varying temperature from 900-1000ºC and at different sintering time of 1-2 h, respectively.

3.2.1 Density of copper- graphite composite

Figure 3.1 illustrates the sintered density of Cu-5wt.% Gr composite with sintering time and temperature. It is observed that with increase in the sintering temperature up to 950ºC and sintering time up to 1.5 h, the density increases which may refer to the enhanced diffusion and particle bonding between atoms of powder particles. Also, higher sintering temperature increases the surface energy of the powder particles, promoting atomic

rearrangement and the neck formation between adjacent particles. This contributes to a more cohesive and denser structure. Further increase in temperature causes a significant decrease in sintered density due to enlargement of the grains of copper matrix. Similarly, density decrement is seen with rise in sintering time at 2 h owing to formation of large size pores at higher holding time.

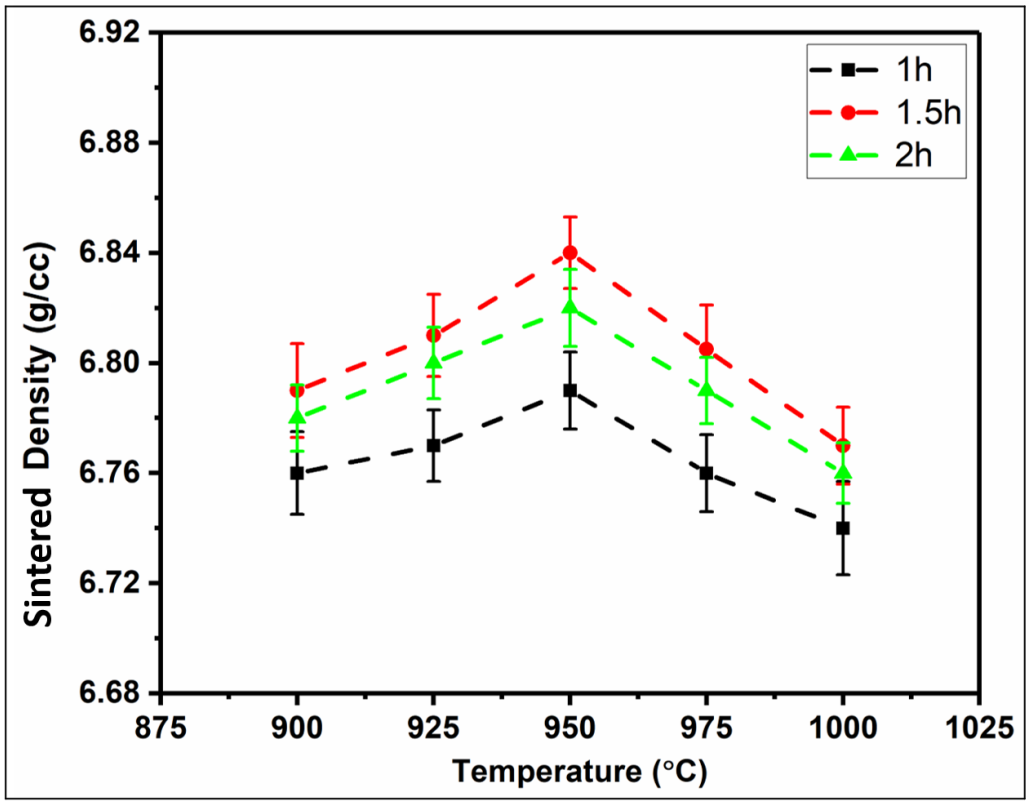

Fig. 3.1 Sintered density of Cu-5wt.% Gr sample with sintering time and temperature

3.2.1 Hardness of copper- graphite composite

Figure 3.2 illustrates the Vickers Hardness Number (VHN) of Cu-5wt.% Gr composite with sintering time and temperature. It is observed that with increase in sintering temperature up to 950ºC and sintering time up to 1.5 h, VHN values increases owing to proper bonding among the powder particles. However, further increase in sintering

temperature and time causes an increase in the size of grains. Coarser grains are formed that results in decrement of hardness of the composite.

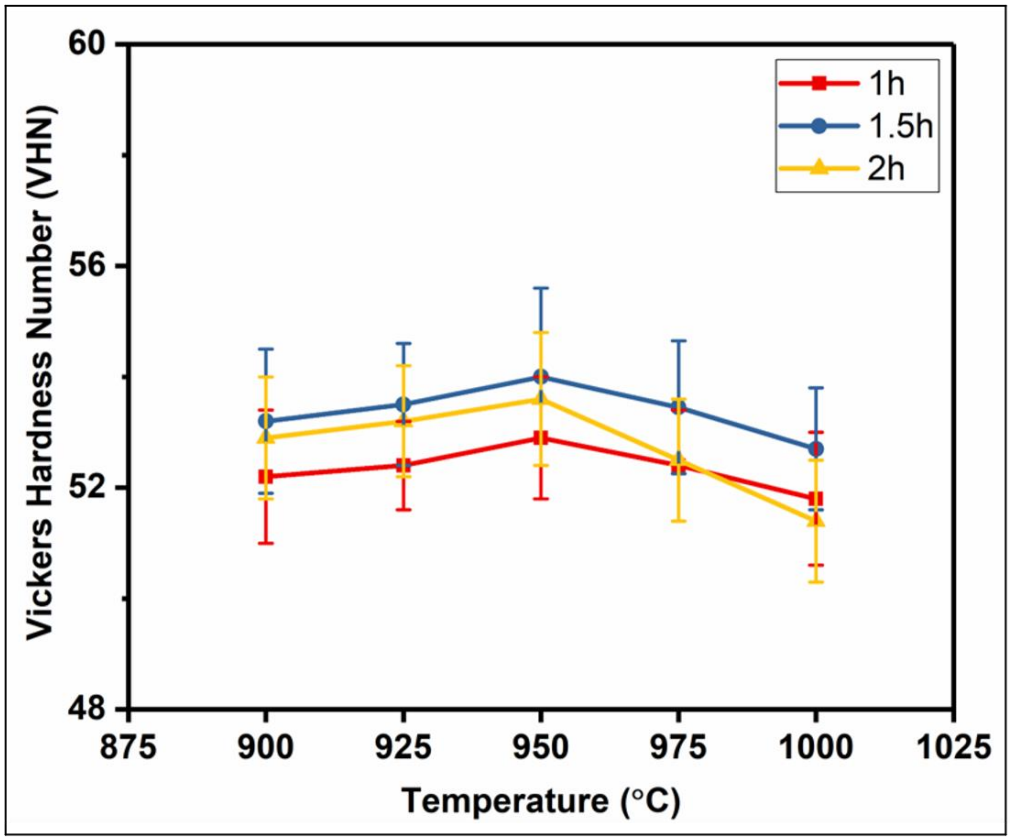

Fig. 3.2 Hardness values of Cu-5wt.% Gr sample with sintering time and temperature

3.3 X-RAY DIFFRACTION (XRD) ANALYSIS

Figure 3.3 illustrates the X-ray diffraction (XRD) pattern for pure copper, along with composites containing different quantities of TiC particles (1.5%, 3.0%, and 4.5% by weight). It is observed that Cu sample consists the peaks of Cu element with strong intensity. However, the Cu-Gr sample shows the peak of C element along with the Cu element peaks which indicates the successfully addition of graphite in the Cu. The TiC reinforced composites depicted Cu element peaks along with the C peaks representing graphite and the TiC peaks. However, the intensity of TiC peaks slightly enhances when TiC content is high. No other phases exist indicating no reaction among the

reinforcements and the atmospheric oxygen. The planes for the respective peaks were also indexed in the XRD image.

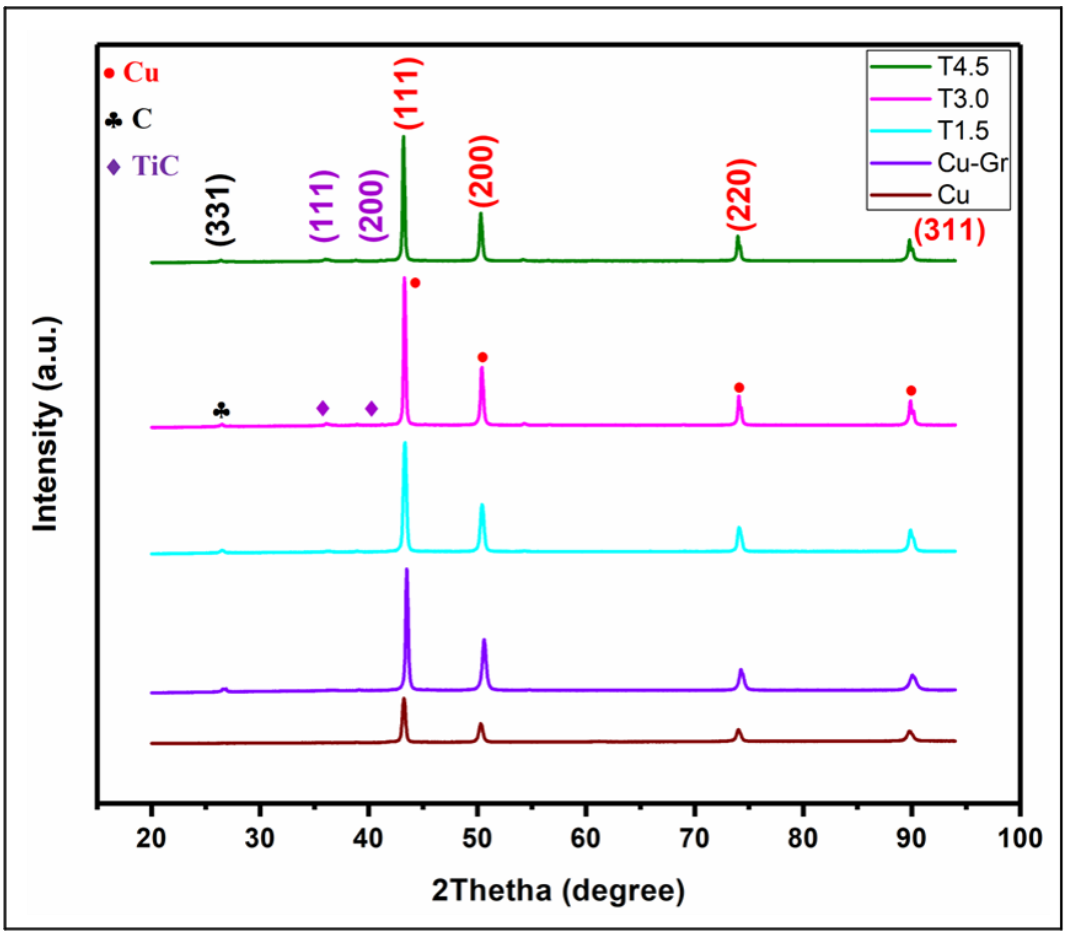

Fig. 3.3 XRD pattern of Cu and composites

3.4 DENSITY AND POROSITY CALCULATION

The densities and the porosity of sintered samples are represented in Fig. 3.4. The theoretical densities of Gr, Cu and TiC are 2.25 g/cm^3, 8.96 g/cm^3 and 4.93 g/cm^3, respectively [C.P. Samal et al., 2013, S. Buytoz et al., 2014]. It was observed that the green and sintered densities of all reinforced composites are less than the sintered pure copper. Since both the reinforcements namely graphite and titanium carbide particles have lower density than pure copper, the green density decreased as the reinforcement content is increased. It was found that the sintered density of the Cu-Gr composite gets

substantially reduced owing to the large variation in the densities of graphite (2.25 g/cm^3) and Cu (8.96 g/cm^3). Additionally, after sintering, trapped gases reduce the weight of the composite samples. The porous nature of composites increases with the rise in the percentage of reinforcements. The rise of porosity value for composites may be due to the improper wetting of reinforcement particles with the copper that results in the formation of voids in the samples. Also, one of the factors of the increase in porosity may be the cluster formation of graphite flakes and as the content of TiC increases, it results in small agglomerations of nano TiC particles which causes rise in porosity.

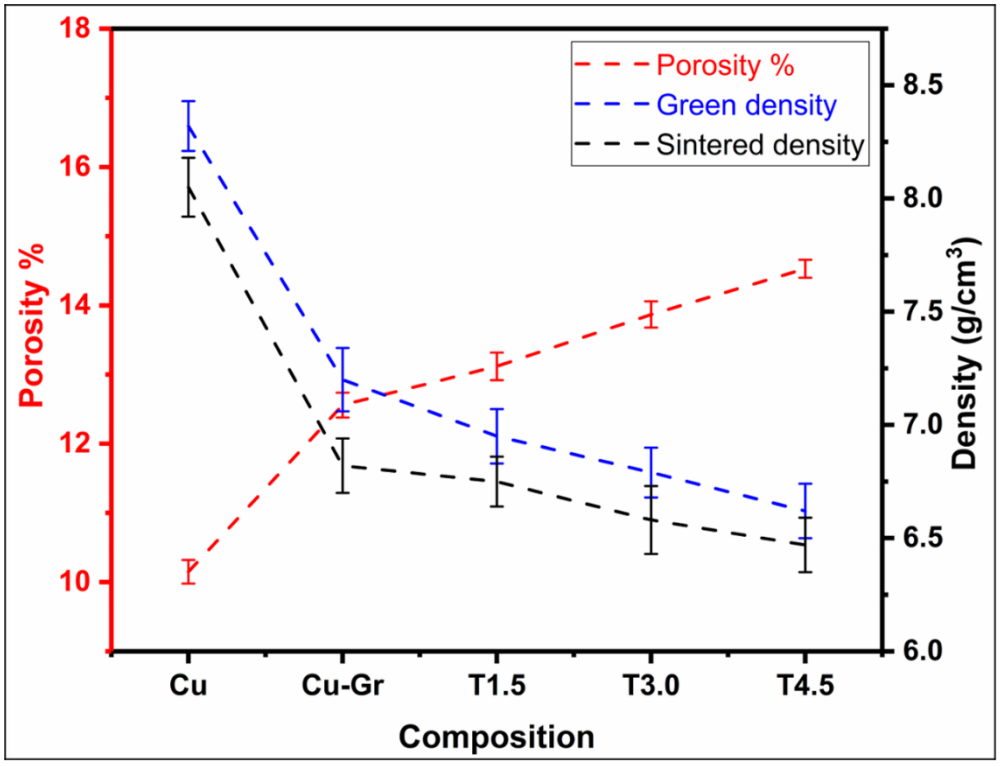

Fig. 3.4 Green density, sintered density and porosity % of Cu and composites

3.5 OPTICAL MICROSCOPY

Figure 3.5 displays the optical micrographs of Cu-Gr composite and Cu-Gr-TiC composites with varying amount of TiC. The optical micrograph Cu-Gr clearly shows the well-defined grain boundaries of Cu along with the graphite particles.

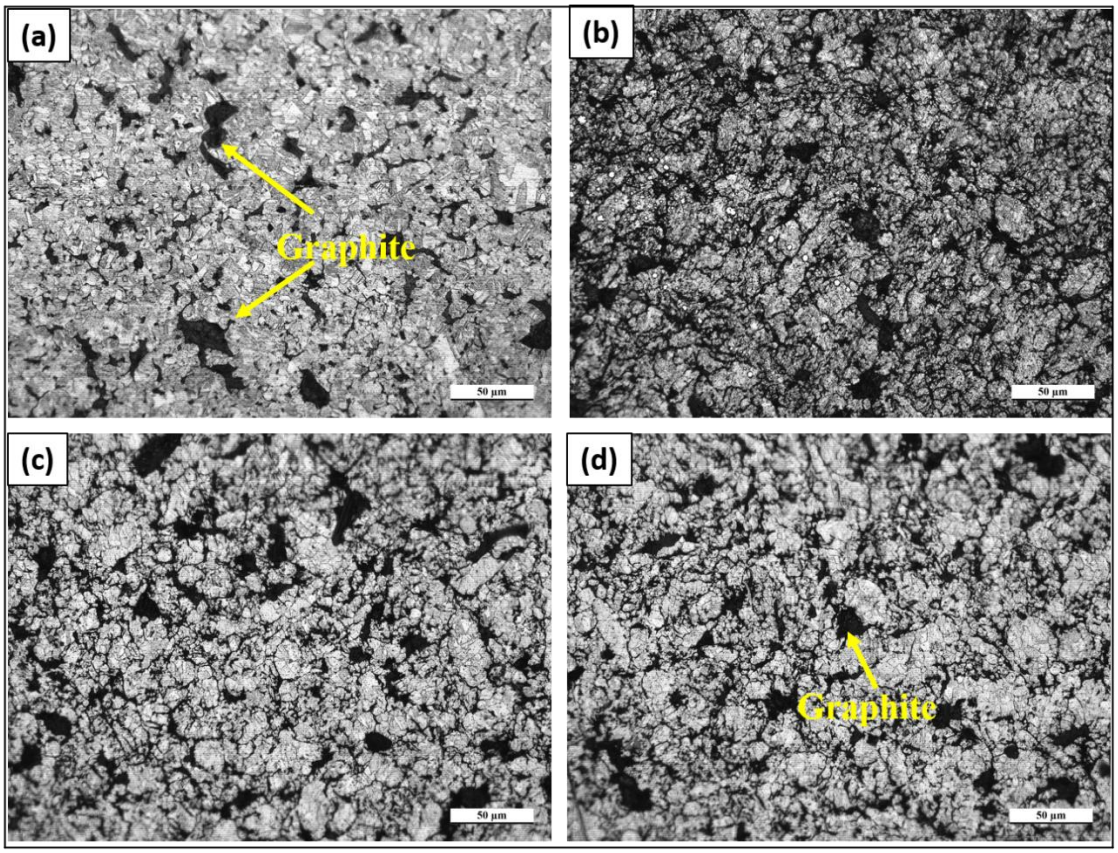

Fig. 3.5 Optical micrographs of sintered composites (a) Cu-Gr, (b) T1.5, (c) T3.0 and (d) T4.5

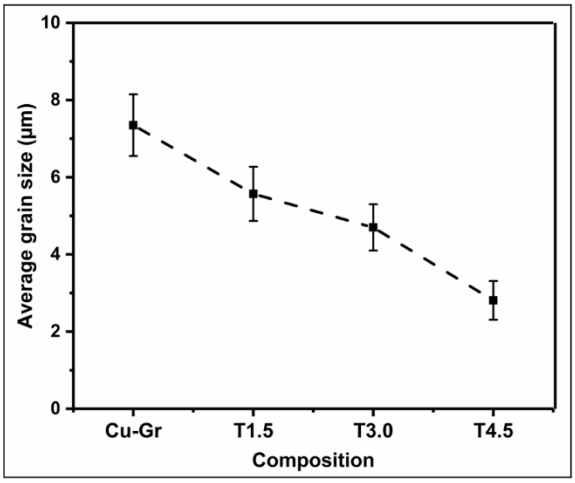

Fig. 3.6 Average grain size of Cu matrix in sintered composites

However, for the TiC reinforced composites, uniform dispersion of graphite particles is observed. The average grain size of Cu matrix grains of all composites is also calculated via linear intercept method as depicted in Fig. 3.6 and the values are 7.35 µm, 5.57 µm,

4.36 μm and 2.81 μm for the Cu-Gr, T1.5, T3.0 and T4.5 composites, respectively. It indicates that with addition of TiC particles in the composite, the average grain size of Cu grains reduces slightly and this reduction increases as amount of TiC particles increase in the composite. The presence of TiC particles suppresses the growth of Cu grains during sintering process.

3.6 SCANNING ELECTRON MICROSCOPY

To understand the effect of milling on the composite powders, FE-SEM images of T4.5 composite powders were taken after subsequent hour of milling. During milling of powders, the hard tungsten carbide balls rotating at high speed of 300 rpm in the vials, impart a high magnitude of kinetic energy to the composite powders. This results in plastic deformation in the shape of powder particles. The prolonged milling causes strain and crack formation in the particles. Due to dry milling the fracturing of particles occurs and simultaneously cold welding may occur due to the heat generated by high speed.

Figure 3.7(a-e) shows the FE-SEM image of composite powders undergoing different hour of milling and Fig. 3.7(f) shows graphite powder at higher magnification and here we observe TiC particles to be cold welded and scattered on the graphite particles due to large surface area provided by graphite particles.

Figure 3.7(a) shows the FE-SEM image of composite powder being milled for 1 hour. The dendritic copper is observed to have extended facets. Collision of powders and balls may result in change in shape of graphite and Cu particles. After 2 hours of ball milling, the composite powder' image is illustrated in Fig. 3.7(b). The facets of Cu are broken down into tiny facets. The TiC particles are distributed over the graphite particles and Cu particles.

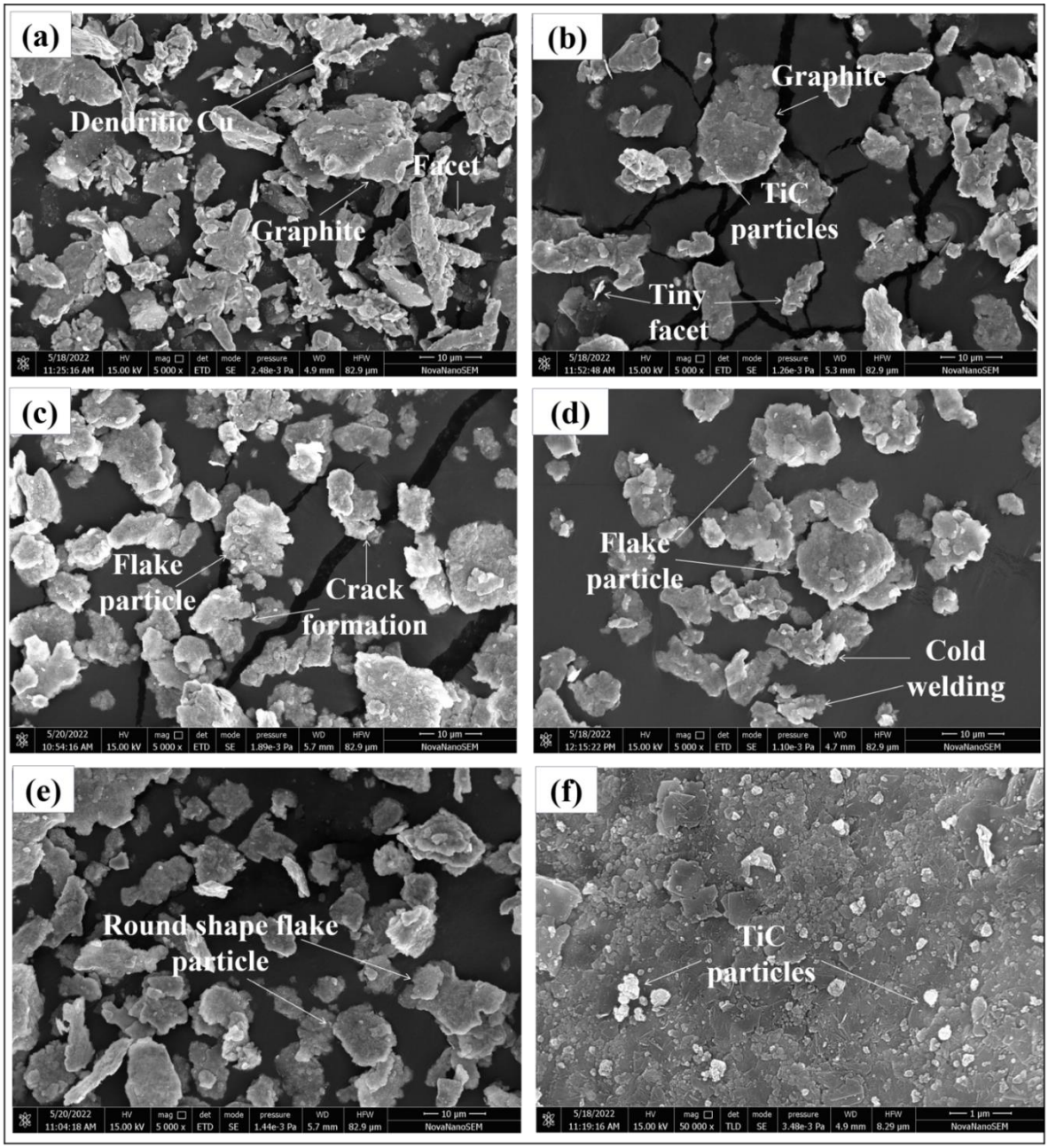

Fig. 3.7 FE-SEM images of T4.5 composite powder after (a) 1 hour milling, (b) 2 hours milling, (c) 3 hours milling, (d) 4 hours milling, (e) 5 hours milling and (f) FE-SEM image of Gr particle at higher magnification

Figure 3.7(c) illustrates the image of milled composite powder after 3 hours. The persistent collision from the grinding balls results in crack formation of powders and the particles become flat. Some of the particles form flake structure having random orientation of the periphery. Figure 3.7(c) depicts the FE-SEM image of milled composite powder after 4 hours. The particles of composite are observed to become flake like

structure with irregular edges. Due to continuous cold welding and fracturing of particles, they develop flake shape morphology [G. Fan et al., 2018, T. Varol et al., 2015]. The FE-SEM image of milled composite powder after 5 hours is illustrated in Fig. 3.7(d). It is found that flake shape particles achieve a near round shape. The milling process results in local fracturing of edges. The Figure 3.7(e) depicts the FE-SEM image of composite powder milled for 5 hours. After 5 h of milling graphite particles are seen to be broken into smaller round shape with irregular edges.

The mechanical and tribological characteristics of a composite are greatly affected by the required uniform dispersion of reinforcements. Therefore, the EDS elemental mapping under SEM of Cu, C, and Ti elements for the sintered composites is done for determining the distribution of reinforcements throughout the composite. Figure 3.8 depicts the SEM images along with EDS elemental mapping of Cu-Gr composite. The EDS elemental mapping of all composites is accomplished in the square region of SEM images. It is seen that in the Cu-Gr sample, the graphite particles are evenly distributed and with some cluster of Gr particles at few locations.

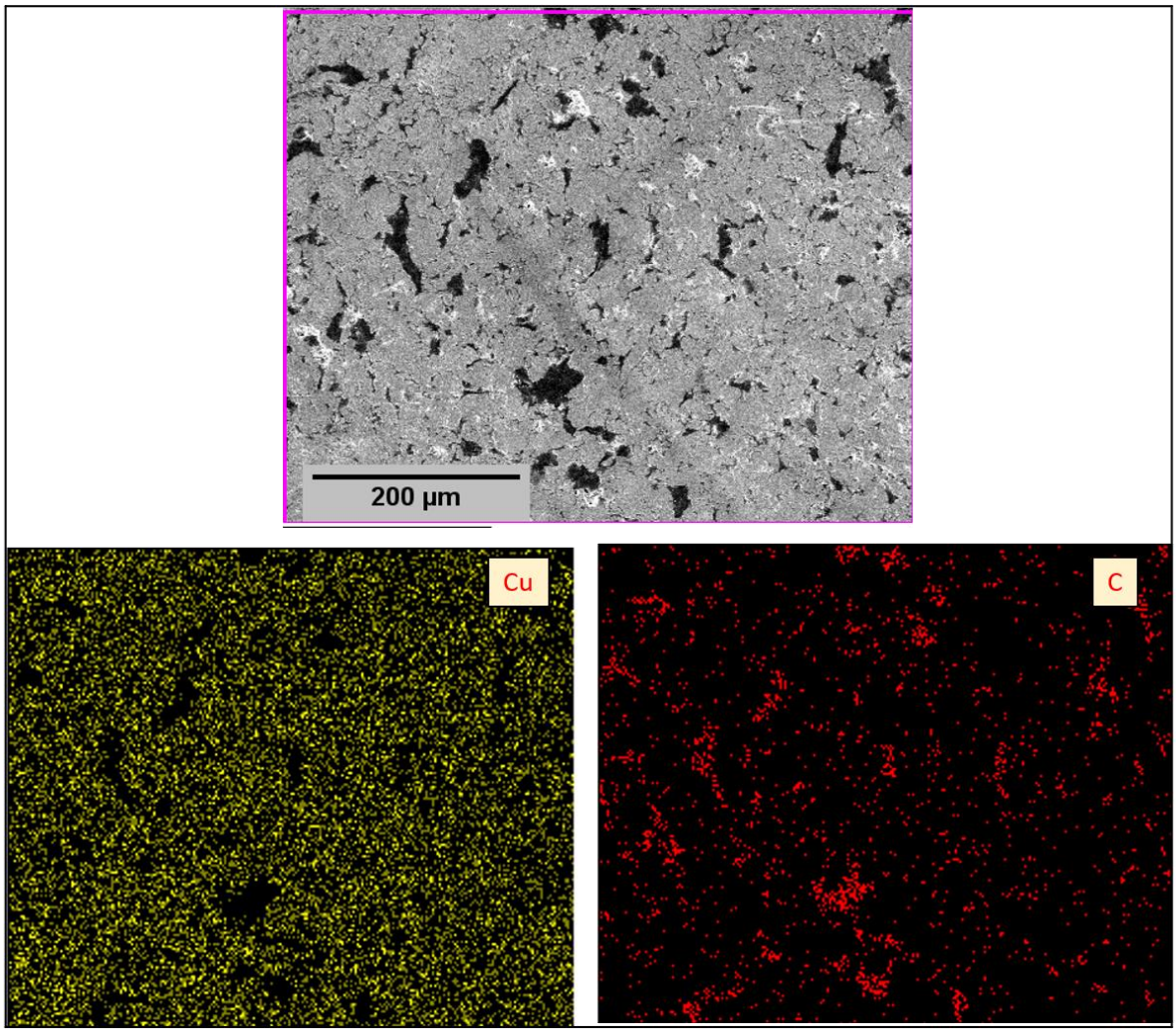

Fig. 3.8 EDS element mapping of Cu and C elements in Cu-Gr composite

Figure 3.9 depicts the SEM images along with EDS elemental mapping of T1.5 composite. The T1.5 composite having TiC particles exhibited enhanced Gr uniformity and refinement. Furthermore, the TiC particles are spread evenly across the T1.5 composite as seen in Fig. 3.9.

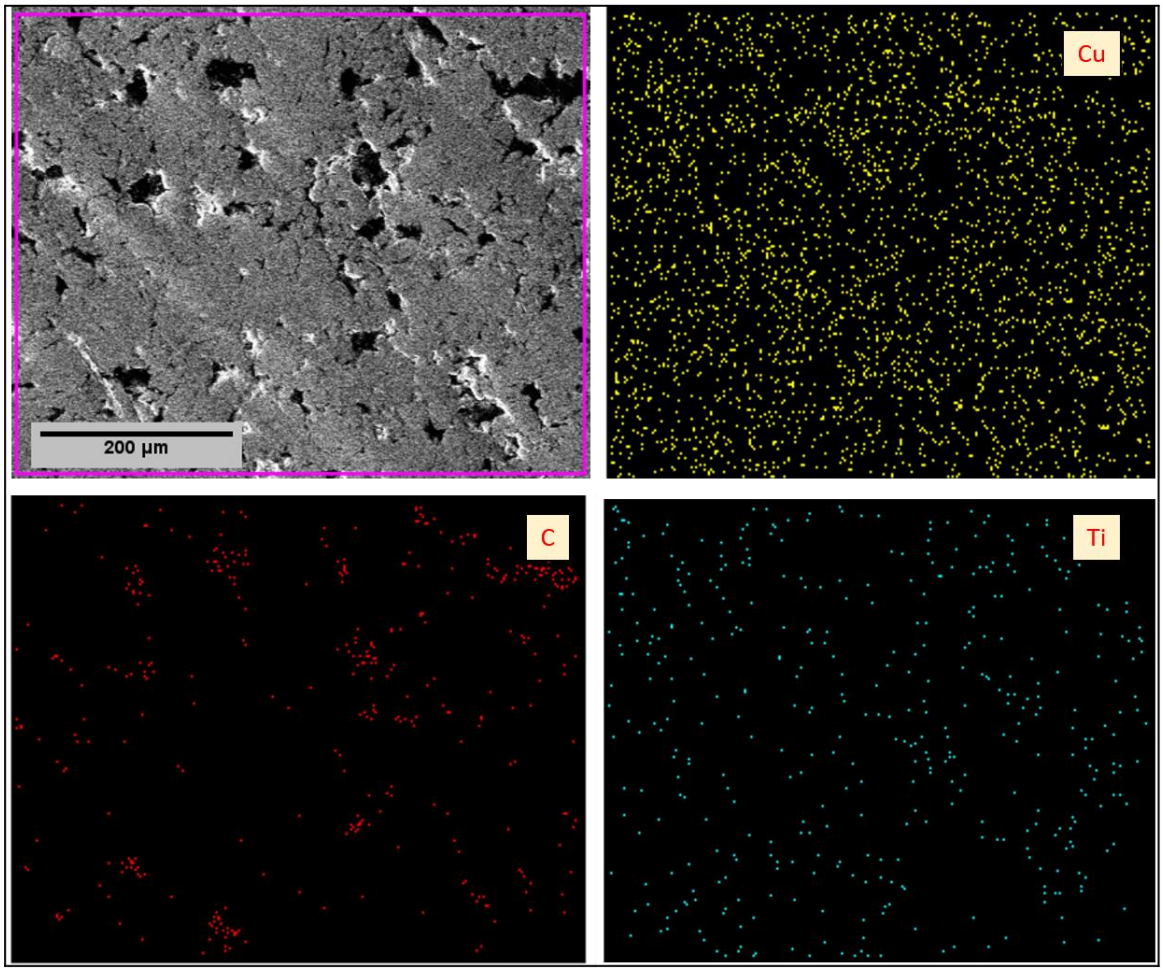

Fig. 3.9 EDS element mapping of Cu, C and Ti elements in T1.5 composite

This distribution of TiC particles is further improved as the amount of TiC particles is raised in the composite (T4.5 composite) as depicted in Fig. 3.10. However, there is also some clustering of TiC particles observed in the T4.5 composite. When the amount of TiC particles in the composite is raised, as shown in Fig. 3.10, the TiC elemental mapping dots are likewise increased which verify the composition of the composites. With more amount of TiC in the composite, the size of graphite cluster also gets reduced. It is because of the hardening nature of TiC particles in the composite and reduces the size of graphite cluster during milling of composites.

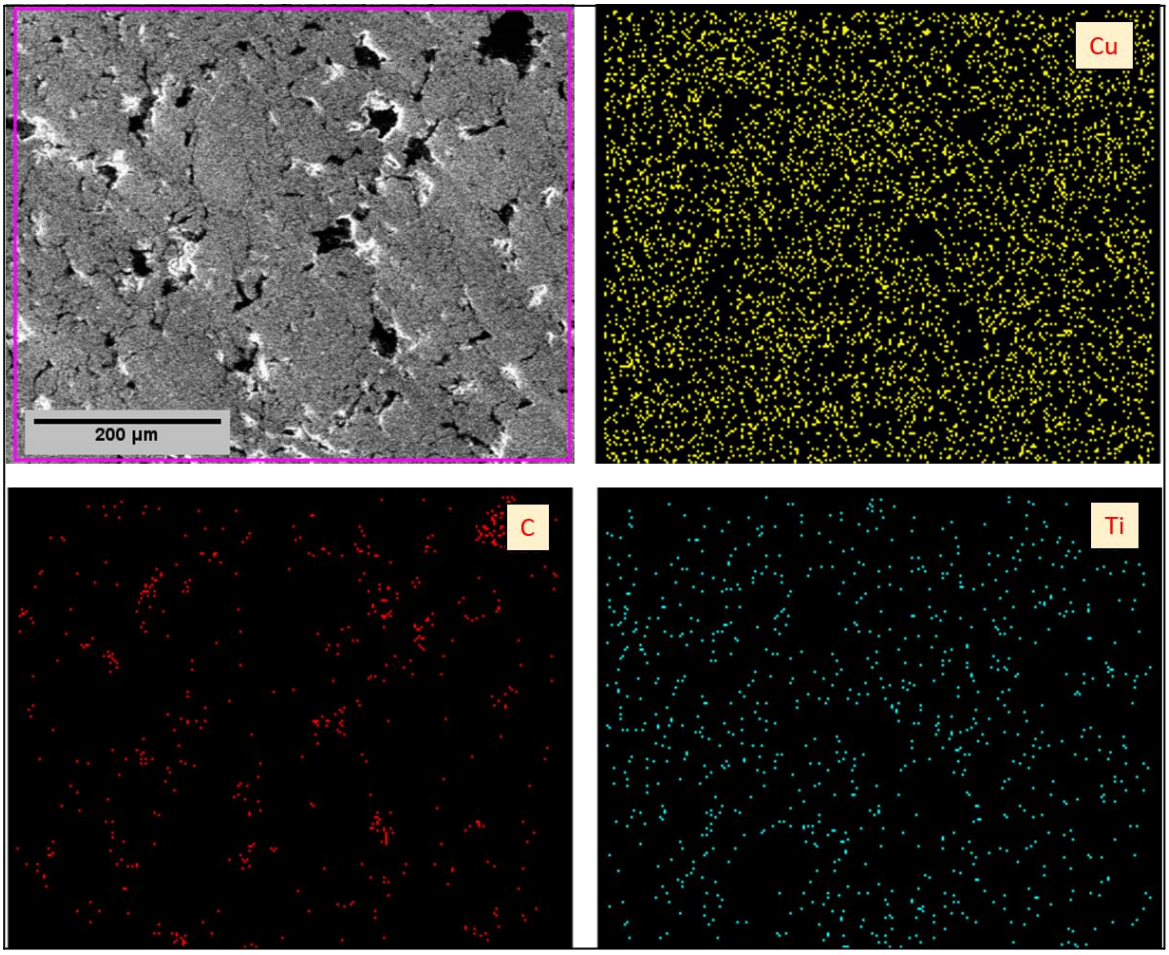

Fig. 3.10 EDS element mapping of Cu, C and Ti elements in T4.5 composite

3.7 MECHANICAL PROPERTIES

The mechanical properties of composite are determined to understand the behaviour of composite under different loading conditions. The variation of Vickers hardness value of Cu and composites is represented in Fig. 3.11(a). It is found that initially the hardness of composite sample decreases on addition of graphite reinforcement particle (Cu-Gr composite), while after this, it continuously increases with addition of TiC reinforcement particles (T1.5 to T4.5 composites). However, maximum hardness of the composite is observed in the T4.5 having 5 wt.% Gr and 4.5 w.t% TiC. Initially decreased hardness of the composite is because of the graphite particles which has soft nature and less hardness than the Cu matrix [M. Kestursatya et a., 2003]. However, the increasing hardness of

composite in the samples (T1.5 to T4.5 composites) is owing to the TiC particles which are hard ceramic particles and they carry the load from the matrix and limit the plastic deformation. Further, these TiC particles restrict the growth of matrix material grains and contribute in enhancing the hardness [P. Sahoo et al., 1991, V.S. Sujith et al., 2019].

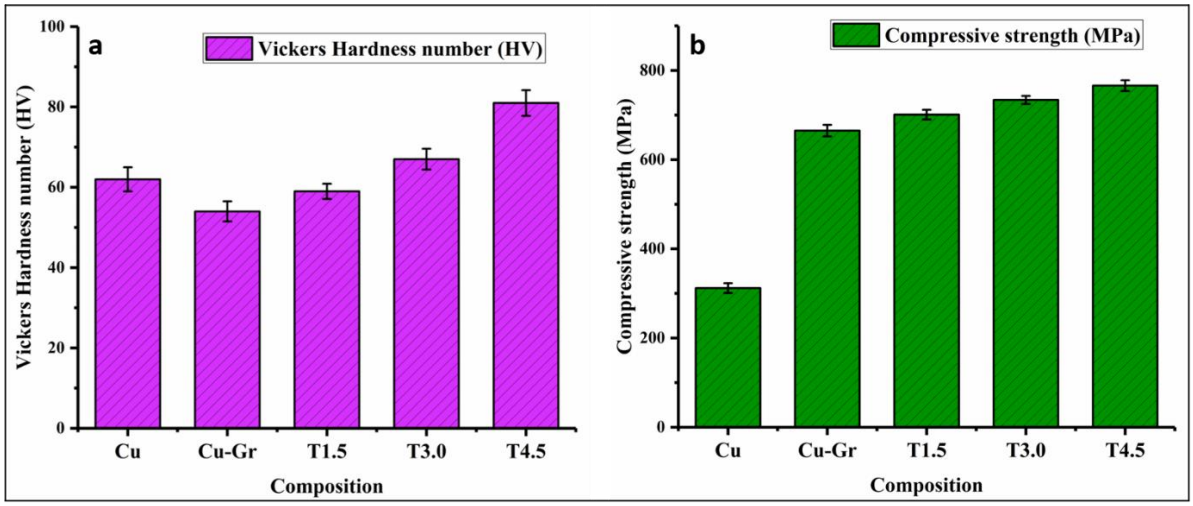

Fig. 3.11 Behaviour of pure Cu and composites for (a) Vickers hardness and (b) Compressive strength

A significant increase in compressive strength is observed with addition of 5 wt.% graphite as displayed in Fig. 3.11(b). The enhanced strength can be credited to the uniform dispersion of particles and the strong bonding at the interface between copper and graphite and that the graphite particles cause an impediment to the movement of dislocation [K.W.H. Seah, 1997]. This obstruction, coupled with the uniform distribution of particles and the strong interfacial bond contributes significantly in compressive strength. Also increasing the TiC concentration leads to a concurrent rise in the compressive strength of the composites. It may be due to several factors. Firstly, the uniform dispersion of the harder TiC particulates within the ductile matrix leads to the reduction in matrix grain size that contributes to the increased strength. The effective transfer of load from the matrix to the particles occurs. The presence of TiC induces a mismatch in the thermal expansion coefficient, resulting in the creation of dislocations,

further contributing to the compressive strength. Moreover, the Orowan strengthening effect, a phenomenon where the movement of dislocations is hindered by the presence of dispersed particles, also contributes to the overall strength of the composites [G. Gautam et al., 2015]. In summary, the synergistic effects of reduced grain size, homogeneous dispersion of TiC, thermal expansion mismatch, load transfer and Orowan strengthening collectively contribute to the observed increase in compressive strength in the composites.

3.8 CONCLUSIONS

The effect of graphite and different TiC compositions on microstructural and mechanical characteristics of Cu-Gr-TiC composites have been studied. The results analysis led to the following conclusions:

- The TiC particles causes slight grain refinement of the Cu matrix. The presence of TiC particles suppresses the growth of Cu grains during sintering process.
- SEM images along with EDS elemental mapping depicts the uniform distribution of graphite and TiC particles. Further, it is seen that finer TiC particles cause clustering of particles at places.
- The T4.5 composite exhibits maximum hardness. The hardness value of this composite is ~50 % more than Cu-Gr composite and ~30% than Cu matrix.
- The compressive strength of Cu increases from 312 to 766 MPa at 4.5 wt.% TiC which is almost 140% more than that of copper.